*chemistry*

MDPI

*Review*

# *m*-Quinodimethane-Based Fused-Ring Diradicals with Singlet and Triplet Ground States

**Akihiro Shimizu**

Division of Chemistry, Department of Materials Engineering Science, Graduate School of Engineering Science, Osaka University, Toyonaka 560-8531, Osaka, Japan; shimizu.akihiro.es@osaka-u.ac.jp

**Abstract:** Diradicals have attracted the attention of chemists due to their unique electronic structures and properties originating from unpaired electrons. One of the fundamental motifs of diradicals is quinodimethane; *p*- and *o*-quinodimethanes are singlet Kekulé hydrocarbons, while *m*-quinodimethane is a triplet non-Kekulé hydrocarbon. Most of the hydrocarbon diradicals studied to date have been limited to *p*- and *o*-quinodimethane-based non-fused-ring and fused-ring open-shell singlet diradicals and *m*-quinodimethane-based non-fused-ring triplet diradicals. In this account, studies on *m*-quinodimethane-based fused-ring diradicals, including an open-shell singlet Kekulé hydrocarbon, an open-shell singlet zwitterion, non-Kekulé hydrocarbon-based triplet diradical and diradical cation, and a triplet Kekulé hydrocarbon, are summarized. They are designed, successfully synthesized, and isolated as crystals, and their fundamental electronic structures and properties have been elucidated by optical, electrochemical, and magnetic measurements, together with DFT calculations. A series of studies showed that controlling the interaction between the two unpaired electrons of *m*-quinodimethane through an appropriate molecular design would produce polycyclic diradicals with various open-shell singlet diradical characters and the energy differences between singlet and triplet states.

**Keywords:** diradicals; quinodimethanes; Kekulé hydrocarbons; non-Kekulé hydrocarbons; polycycles

check for updates

Academic Editor: Ryan C. Fortenberry

Received: 10 February 2025
Revised: 7 March 2025
Accepted: 11 March 2025
Published: 13 March 2025

**Citation:** Shimizu, A. *m*-Quinodimethane-Based Fused-Ring Diradicals with Singlet and Triplet Ground States. *Chemistry* **2025**, *7*, 40. https://doi.org/10.3390/chemistry7020040

**Copyright:** © 2025 by the author. Licensee MDPI, Basel, Switzerland. This article is an open access article distributed under the terms and conditions of the Creative Commons Attribution (CC BY) license (https://creativecommons.org/licenses/by/4.0/).

## 1. Introduction

Diradicals have attracted the attention of chemists as magnetic, electrochemical, and optical materials due to their unique electronic structure and physical properties derived from two unpaired electrons [1]. When the two unpaired electrons of a diradical interact, the electron spins become antiparallel due to the bonding interaction, resulting in a singlet ground state, or the electron spins become parallel due to the ferromagnetic interaction, resulting in a triplet ground state. Establishing a method to control these interactions is essential to create diradicals with different ground spin multiplicities, unique electronic states, and physical properties.

One of the fundamental diradical skeletons is quinodimethane (Figure 1a). *p*- and *o*-quinodimethanes are open-shell singlet Kekulé hydrocarbons, while *m*-quinodimethane is a triplet non-Kekulé hydrocarbon. Most open-shell singlet hydrocarbon diradicals are *p*-quinodimethane-based Kekulé hydrocarbons, described as the resonance of the closed-shell and diradical structures (Figure 1b) [2–9]. A variety of studies have been conducted on hydrocarbon diradicals, spanning from non-fused-ring hydrocarbons, including Thiele's hydrocarbons [10] and Tschitschibabin's hydrocarbons [11,12], to fused-ring hydrocarbons, including biphenalenyls [13–17], zethrenes [18–24], and indeno fluorenes [25–28]. The scope of study also extends to *o*-quinodimethane-based open-shell singlet

Kekulé hydrocarbons (Figure 1c), such as 9,10-bis(di-(*p*-methoxyphenyl)methylene)-9,10-dihydrophenanthrene [29] and indeno[2,1-*a*]fluorene derivatives [30], serving as notable examples of non-fused-ring and fused-ring hydrocarbons, respectively.

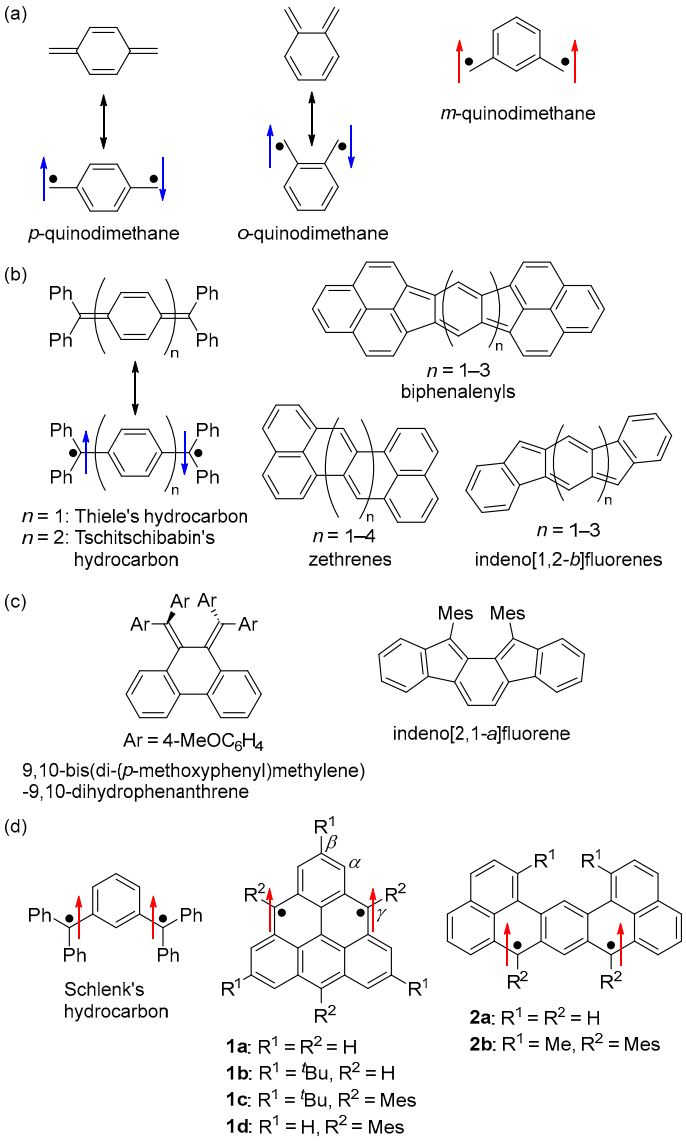



**Figure 1.** Structures of (**a**) quinodimethanes, (**b**) *p*-quinodimethane-based and (**c**) *o*-quinodimethane-based open-shell singlet hydrocarbons, and (**d**) *m*-quinodimethane-based triplet hydrocarbons. Arrows indicate electron spin (blue and red colors are for singlet and triplet diradicals, respectively). Mes = 2,4,6-$Me_3C_6H_2$.

On the other hand, *m*-quinodimethane-based triplet non-fused-ring non-Kekulé hydrocarbons have long been studied. Schlenk's hydrocarbon [31,32], synthesized in 1915, is a typical example (Figure 1d). Rajca et al. synthesized and isolated a kinetically stabilized Schlenk's hydrocarbon derivative [33,34]. Fused-ring *m*-quinodimethane-based triplet hydrocarbons, such as triangulene (**1a**) [35–37] and dibenzo[*de*,*jk*]pentacene (**2a**) [21,38], have also been studied (Figure 1d). However, due to their high reactivity and instability, these diradicals have not been isolated, nor have their physical properties been clarified in detail.

Based on these backgrounds, we focused on *m*-quinodimethane, considering that by controlling the magnitude of the interaction between the two unpaired electrons through appropriate molecular design, not only the energy difference between the singlet and

triplet states ($\Delta E_{ST}$) but also the ground spin multiplicity of diradicals could be controlled. Such spin multiplicity control is not applicable to *p*- and *o*-quinodimethane, which have singlet ground states. We designed and synthesized the following *m*-quinodimethane-based polycyclic diradicals: (1) an open-shell singlet Kekulé hydrocarbon, (2) an open-shell singlet zwitterion, (3) a non-Kekulé hydrocarbon-based triplet diradical and diradical cation, and (4) a triplet Kekulé hydrocarbon [39].

## 2. Open-Shell Singlet Kekulé Hydrocarbon

When we started this study in 2010, there was no study of *m*-quinodimethane-based open-shell singlet Kekulé hydrocarbons. We then designed indeno[2,1-*b*]fluorene (**3a**), an isomer of indenofluorenes (Figure 2a) [40]. Although no Kekulé structure can be drawn to *m*-quinodimethane, a Kekulé structure could be drawn to **3a**. The singlet state of **3a** is stabilized because of the bonding interaction between the two unpaired electrons through the outer benzene ring. Considering the resonance structures of **3a**, the Kekulé structure is stabilized by the bond formation and one Clar's aromatic sextet (benzene rings shown in the bold line), while the singlet diradical structure is stabilized by three Clar's aromatic sextets. Therefore, **3a** would comprise the contribution of both structures and have an open-shell singlet diradical character.

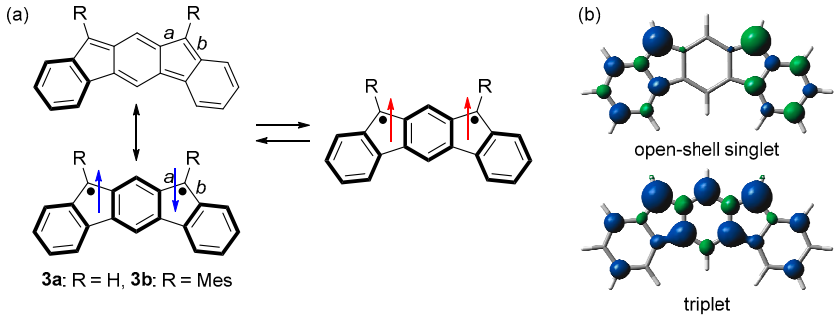
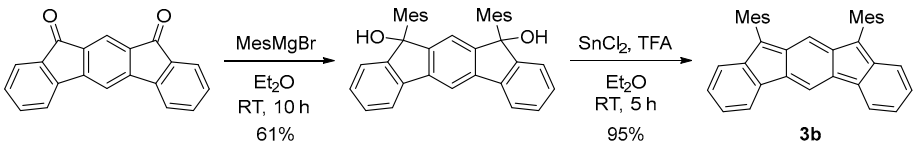



**Figure 2.** (**a**) Resonance structures of **3**. Arrows indicate electron spin (blue and red colors are for singlet and triplet diradicals, respectively). (**b**) Spin densities of open-shell singlet and triplet states of **3a**. Blue and green surfaces represent α and β spin densities, respectively.

DFT calculations predicted that **3a** has a singlet ground state with an open-shell singlet diradical character of 0.71 (LC-UBLYP/6-311G(d,p)//UB3LYP/6-311G(d,p)) and $\Delta E_{ST}$ of $-11.3$ kJ mol$^{-1}$ (UB3LYP/6-311G(d,p)). The spin density distributions were predicted to be similar to those of the two benzyl radicals in the singlet state and *m*-quinodimethane in the triplet state (Figure 2b). Unlike *p*- and *o*-quinodimethane-based open-shell singlet Kekulé hydrocarbons, the spin density distributions of **3a** in the singlet and triplet states are quite different because the triplet state is stabilized by *m*-quinodimethane moiety.

We designed and synthesized a derivative **3b** by introducing mesityl groups for kinetic stabilization (Scheme 1 and Figure 2a). **3b** was found to be stable enough to be purified by column chromatography. Single crystals of **3b** were obtained by recrystallization from acetonitrile solution in a degassed sealed tube (Figure 3a). Bonds *a* (1.437 Å) and *b* (1.431 Å) are longer than the C(sp$^2$)–C(sp$^2$) bond of benzene (1.39 Å), indicating the contribution of the diradical structure in addition to the Kekulé structure (Figure 2a).




**Scheme 1.** Synthesis of **3b**.

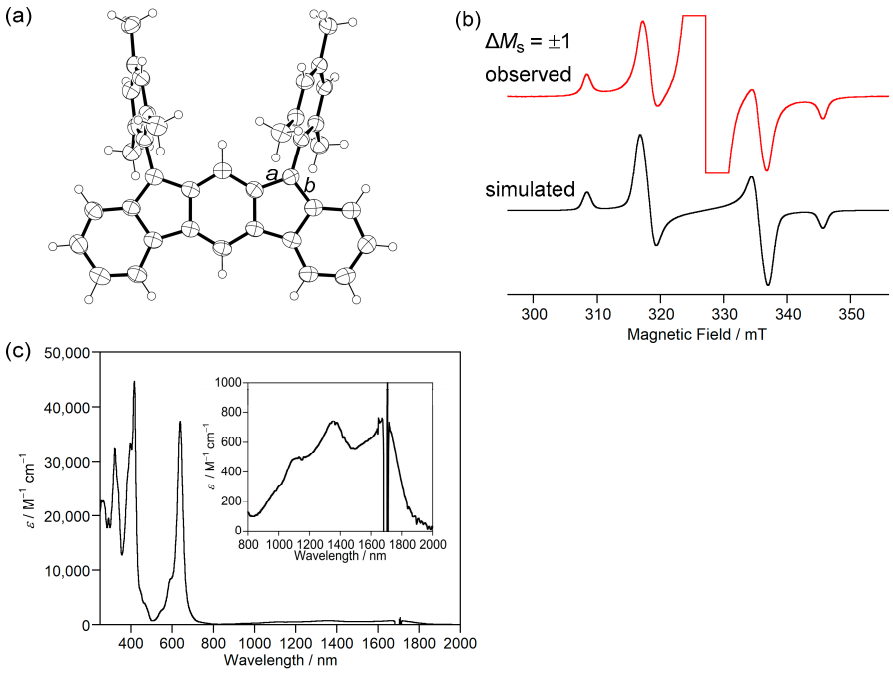



**Figure 3.** (**a**) ORTEP drawing of **3b**. Displacement ellipsoids are drawn at the 50% probability level. (**b**) ESR spectrum of **3b**. (**c**) UV-Vis-NIR absorption spectra of **3b** in $CH_2Cl_2$. Reprinted with permission from Ref. [40], Wiley-VCH, 2013.

ESR measurements showed a signal with a $|D|$ value of 0.017 $cm^{-1}$ originating from the thermally excited triplet state of **3b** (Figure 3b). Due to the small energy difference between HOMO and LUMO, **3b** exhibits absorption in the near-infrared (NIR) region of ca. 1700 nm in $CH_2Cl_2$ (Figure 3c), although **3b** has only 20 $\pi$ electrons in its main core structure. **3b** is the first example of a *m*-quinodimethane-based open-shell singlet Kekulé hydrocarbon. This study introduced new aspects of open-shell singlet Kekulé hydrocarbon and led to the study of fluoreno[2,3-*b*]fluorene [41] and dianthraceno[2,3-*a*:3′,2′-*h*]-*s*-indacene [42].

## 3. Open-Shell Singlet Zwitterion

In contrast to the numerous studies of open-shell singlet Kekulé hydrocarbons, few studies were conducted on the open-shell singlet zwitterions, which were described as the resonance of the zwitterionic and diradical structures. This means that many aspects of their electronic structures and physical properties are unresolved [43,44].

We designed azoniadibenzo[*a*,*j*]phenalenide (**4a**), in which *m*-quinodimethane is bridged by diphenylamine (Figure 4a) [45]. DFT calculations predicted that **4a** has a singlet ground state with an open-shell singlet diradical character of 0.57 (LC-UBLYP/6-311G(d,p)//UB3LYP/6-311G(d,p)) and $\Delta E_{ST}$ of −24.0 kJ $mol^{-1}$ (UB3LYP/6-311G(d,p)). The spin density distribution was predicted to be similar to that of **3a**; spins delocalize over two benzyl radicals in the singlet state and *m*-quinodimethane moiety in the triplet state (Figure 4b).

We designed and synthesized a derivative **4b** with *tert*-butyl and mesityl groups for kinetic stabilization (Scheme 2, Figure 4a). Single crystals of **4b** were obtained by recrystallization from tetrahydrofuran–hexane solution in a degassed sealed tube (Figure 5a). Unlike the open-shell singlet Kekulé hydrocarbons such as **3b**, there was no significant difference in the bond length between the singlet ground state and the thermally excited triplet state of **4b** (Figure 5a), and thus, its open-shell singlet diradical character could not be clarified based on the bond length.

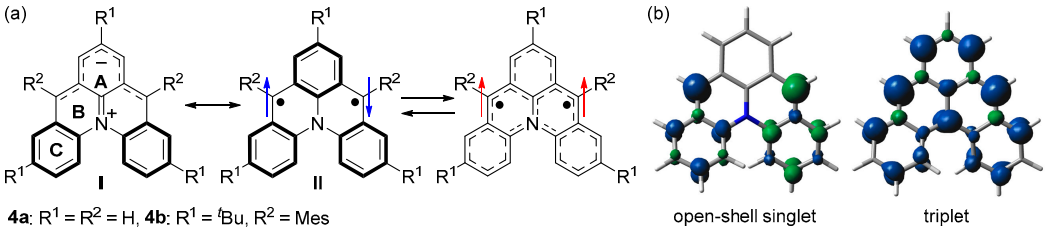
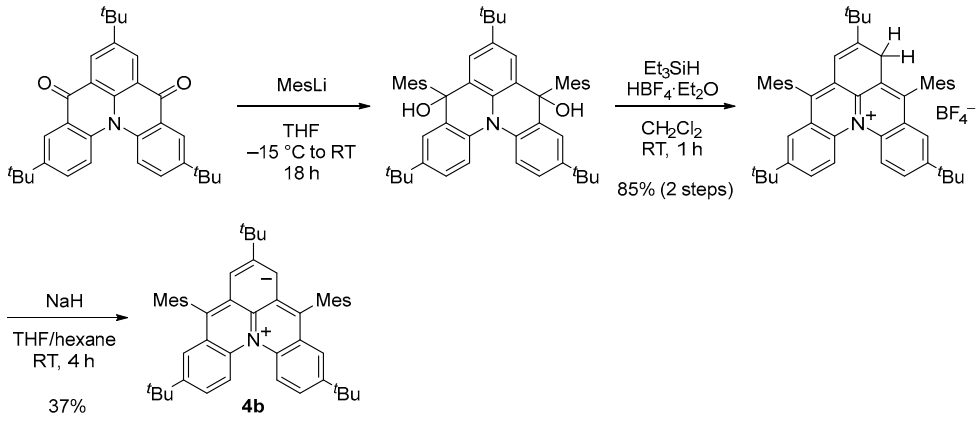



**Figure 4.** (**a**) Resonance structures of **4**. Arrows indicate electron spin (blue and red colors are for singlet and triplet diradicals, respectively). (**b**) Spin densities of open-shell singlet and triplet states of **4a**. Blue and green surfaces represent α and β spin densities, respectively.




**Scheme 2.** Synthesis of **4b**.

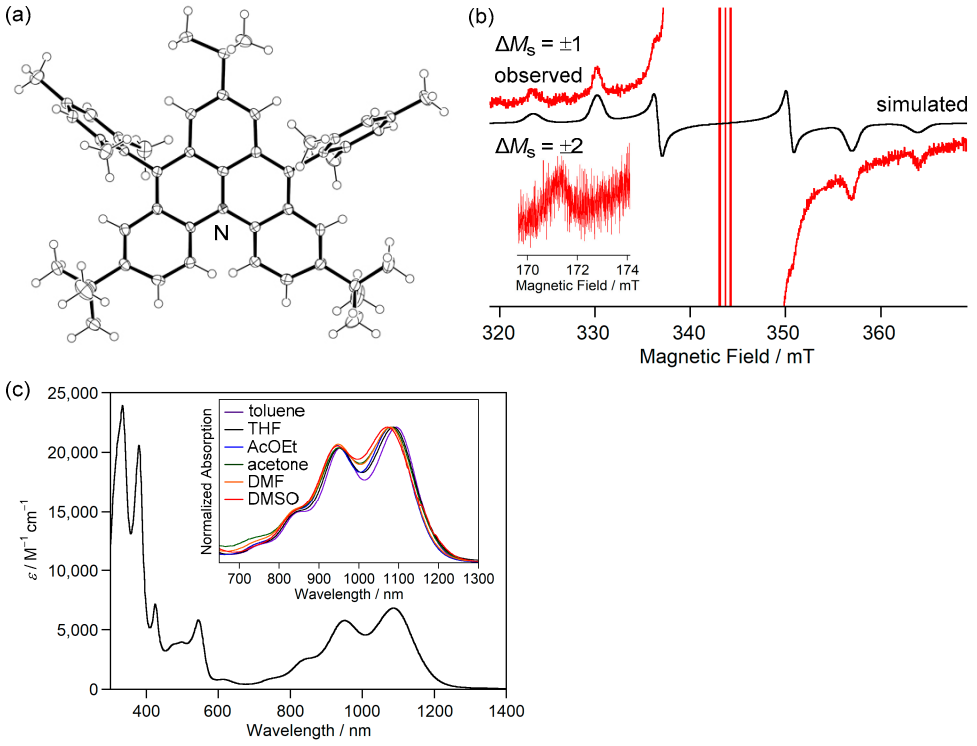



**Figure 5.** (**a**) ORTEP drawing of **4b**. Displacement ellipsoids are drawn at the 50% probability level. (**b**) ESR spectra of **4b** at 470 K. (**c**) UV-Vis-NIR spectra of **4b** in THF. Reprinted with permission from Ref. [45], Wiley-VCH, 2019.

To clarify the electronic structure, we focused on aromaticity. HOMA (Harmonic Oscillator Model of Aromaticity) values [46,47], Nucleus-Independent Chemical Shift (NICS) values [48–50], and Anisotropy of the Induced Current Density (ACID) plot [51,52]

showed that rings **A** and **C** are aromatic, while ring **B** is non-aromatic. The chemical shifts of the $^1$H NMR spectra revealed that the negative charge is delocalized over the upper part of **4b**, indicating the contribution of the zwitterionic structure **I** (Figure 4a).

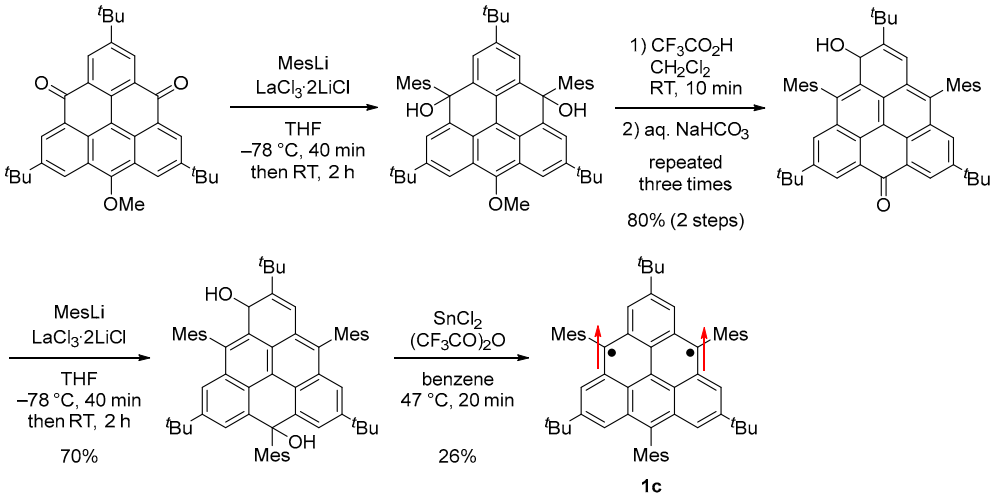
ESR measurements were conducted to experimentally clarify the open-shell singlet diradical character of **4b**. An ESR signal with a $|D|$ value of 0.019 cm$^{-1}$ originating from the thermally excited triplet state of **4b** was observed (Figure 5b). The $\Delta E_{ST}$ was determined to be −36.4 kJ mol$^{-1}$ by variable-temperature ESR spectra. These results showed that **4b** is described as the resonance of the zwitterionic structure **I** and diradical structure **II** (Figure 4a).

**4b** showed an absorption band in the NIR region of 1086 nm in tetrahydrofuran, indicating a small energy difference between HOMO and LUMO (Figure 5c). Despite the contribution of the zwitterionic structure, the absorption wavelength did not significantly depend on the polarity of solvents, probably because of the small dipole moment. Therefore, open-shell singlet zwitterions with large dipole moments are required to respond to various external stimuli. A careful molecular design is required because the zwitterionic structure significantly stabilizes the singlet state, as observed in the study of bis-periazulene (cyclohepta[*def*]fluorene) [53].

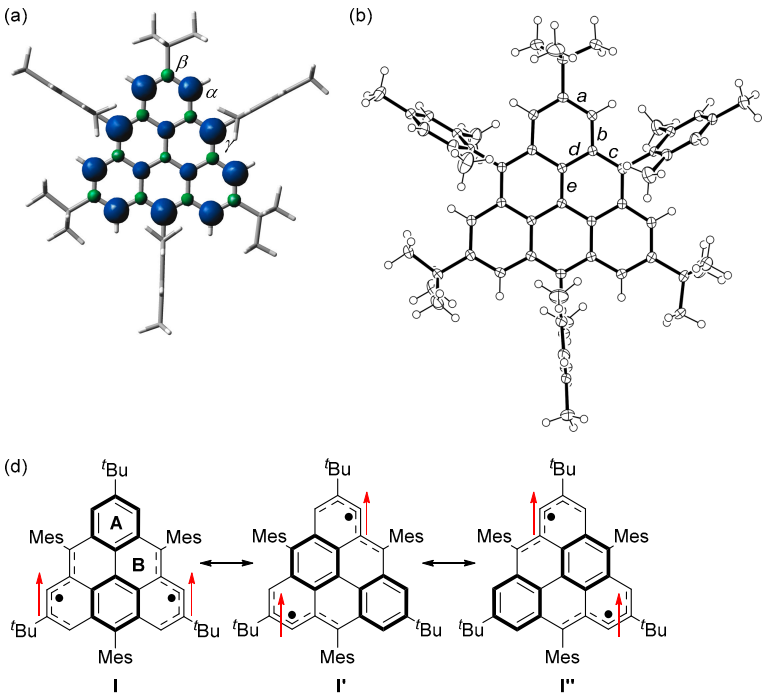
## 4. Non-Kekulé Hydrocarbon-Based Triplet Diradical and Diradical Cation

The first attempted synthesis of triangulene (**1a**), a fused-ring triplet non-Kekulé hydrocarbon, was conducted by Clar et al. in 1953, but **1a** was highly reactive and polymerized at low temperatures [35,36]. A kinetically stabilized derivative **1b** was designed and generated by Nakasuji et al. in 2001, and its triplet ground state was experimentally confirmed [37]. However, **1b** was not isolated due to its high reactivity. Recently, many unstable triplet diradicals have been generated on metal surfaces and observed using STM and AFM. **1a** and **2a** were reported by Gross et al. in 2017 [54] and Wang et al. in 2020 [55], respectively. However, due to the influence of metals, the fundamental optical, electrochemical, and magnetic properties of these radicals have not been elucidated.

Because **1b** [37] polymerized at γ carbons with a large spin density, we designed and synthesized **1c** by introducing mesityl groups at the γ carbons for kinetic stabilization (Scheme 3, Figures 1d and 6a) [56]. **1c** was stable in solution at room temperature in a degassed sealed tube and in the solid state in a glove box under an argon atmosphere but gradually decomposed when the solution was exposed to air.




**Scheme 3.** Synthesis of **1c**. Arrows indicate electron spin.




| bond | obs (Å) | calc (Å) | WBI |
|---|---|---|---|
| *a* | 1.395* | 1.396* | 1.399* |
| *b* | 1.421* | 1.420* | 1.263* |
| *c* | 1.419* | 1.422* | 1.274* |
| *d* | 1.429* | 1.430* | 1.210* |
| *e* | 1.418* | 1.419 | 1.237 |

**Figure 6.** (**a**) Spin densities of the triplet state of **1c**. Blue and green surfaces represent α and β spin densities, respectively. (**b**) ORTEP drawing of **1c**. Displacement ellipsoids are drawn at the 50% probability level. (**c**) Observed and calculated bond lengths and calculated Wiberg bond indices (WBI) of **1c**. * Mean value. (**d**) Resonance structures of **1c**. Arrows indicate electron spin. Reprinted with permission from Ref. [56], American Chemical Society, 2021.

Single crystals of **1c** obtained by recrystallization from a $CH_2Cl_2$–hexane solution in a degassed sealed tube had an almost $D_{3h}$ symmetric main core structure with no significant bond length alternation based on the bond lengths and Wiberg bond indices [57] (Figure 6c). The HOMA and NICS(1)$_{zz}$ values and the ACID plot indicate that rings **A** and **B** are aromatic. Therefore, the canonical structure **I** with two Clar's aromatic sextets contributes significantly, and **I′** and **I″** also contribute equally due to the molecular symmetry (Figure 6d).

ESR spectra of the toluene solution of **1c** at room temperature showed an ESR signal split by six α-protons (Figure 7a). The experimental spin density of α-carbon atoms (0.293) agreed well with the calculated spin density (+0.279, UBLYP/6-311G(d)//UB3LYP/6-311G(d)) (Figure 6a). These results indicate that the two unpaired electrons of **1c** are mainly delocalized over the periphery of the main core structure, with 54% (9% per carbon atom) in the six α carbons and 33% (11% per carbon atom) in the three γ carbons.

The ESR spectrum of the frozen toluene solution of **1c** did not show the characteristic fine structure of the triplet species and showed a very weak forbidden transition of $\Delta M_s = \pm 2$. Although the reason for these phenomena is unclear, the triangulene derivative **1d**, which was reported by Juríček et al., also did not show the fine structure of the transition of $\Delta M_s = \pm 1$ and the forbidden transition at $\Delta M_s = \pm 2$ [58]. The triplet state of **1c** was confirmed by a two-dimensional electron spin transient nutation (2D-ESTN) spectrum of a frozen toluene solution of **1c** (Figure 7b) [59,60]; the signals at the nutation frequencies of 26.8 and 19.0 MHz were attributed to the triplet state of **1c** and a small amount of monoradical impurity, respectively, because the ratio was $2^{1/2}$:1.

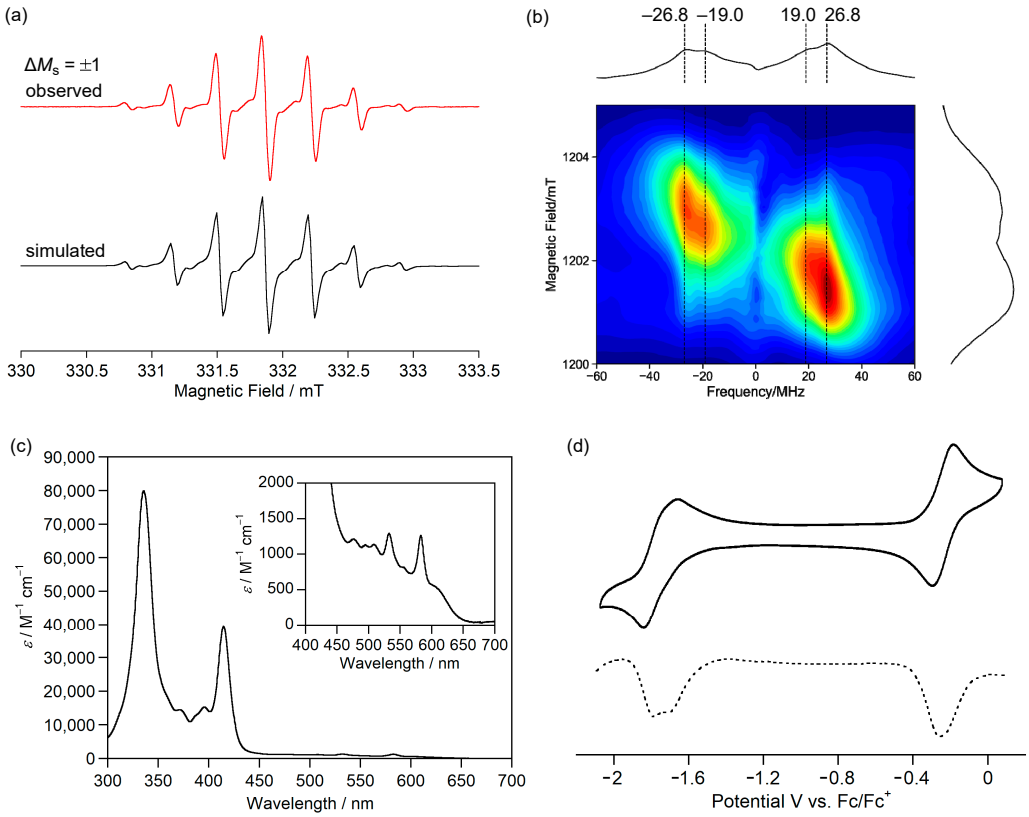



**Figure 7.** (**a**) X-band cw ESR spectra of **1c** in toluene at room temperature (red, experiment; black, simulation). (**b**) Q-band pulse ESR-based two-dimensional electron spin transient nutation spectra of **1c** in frozen toluene solution at 50 K. (**c**) UV-Vis absorption spectrum of **1c** in $CH_2Cl_2$. (**d**) Cyclic voltammogram (solid line) and differential pulse voltammogram (dashed line) of **1c** in $CH_2Cl_2$. Reprinted with permission from Ref. [56], American Chemical Society, 2021.

Magnetic susceptibility measurements showed that $\chi_p T$ of **1c** was 0.88 emu K mol$^{-1}$, which is larger than the theoretical value (0.75 emu K mol$^{-1}$) of the singlet diradical. The $\chi_p T$ value was constant at 10–300 K, indicating that **1c** has a triplet ground state with a large $\Delta E_{ST}$, as expected from the calculated $\Delta E_{ST}$ of +53.5 kJ mol$^{-1}$ (UB3LYP/6-311G(d,p)).

The fundamental optical and electrochemical properties of **1c** were elucidated by measuring the UV-Vis absorption spectrum and cyclic voltammogram. **1c** exhibited weak absorption bands at 450–600 nm in $CH_2Cl_2$ (Figure 7c), which were assigned to transitions from α-HOMO to α-LUMO and β-HOMO to β-LUMO. **1c** in dichloromethane showed a reversible two-electron oxidation wave to dication and reversible two-stage one-electron reduction waves to radical anion and dianion (Figure 7d). The small differences between the first and second oxidation potentials and between the first and second reduction potentials are consistent with the degenerated α-HOMOs (–4.50 eV) and β-LUMOs (–2.55 eV). **1c** is the first hydrocarbon with a triplet ground state isolated in crystalline forms.

We also designed and synthesized a nitrogen-doped triangulene cation derivative **5b**$^+$·TfO$^-$ with *tert*-butyl groups for kinetic protection, which is isoelectronic to **1c** (Figure 8 and Scheme 4) [61]. During our study, Wang et al. generated **5a**$^+$ on Au surface and elucidated its triplet ground state [62], but its optical, electrochemical, and detailed magnetic properties remain to be elucidated.

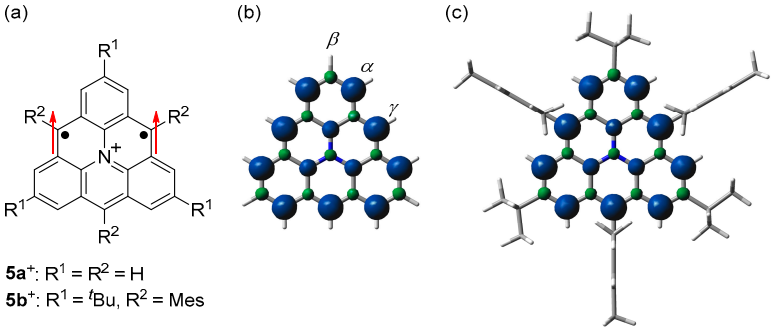
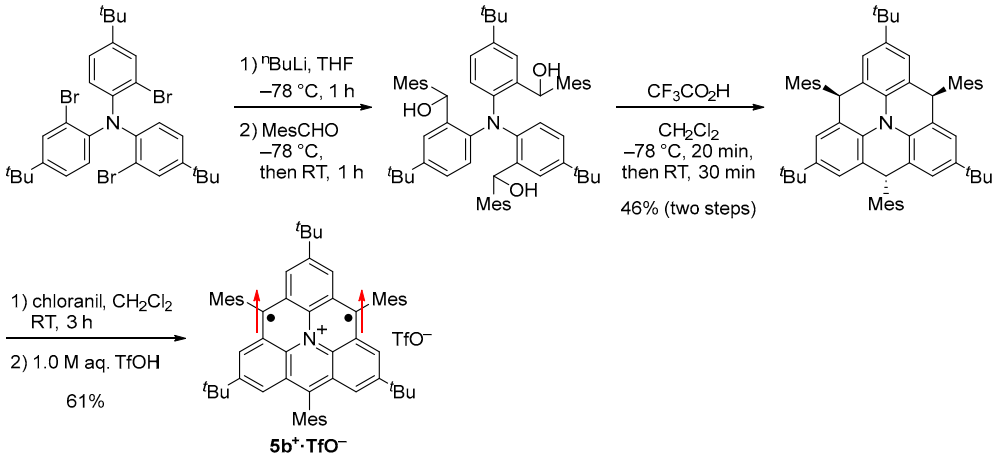



**Figure 8.** (**a**) Structures of **5**$^{+}$. Arrows indicate electron spin. Spin densities of triplet states of (**b**) **5a**$^{+}$ and (**c**) **5b**$^{+}$. Blue and green surfaces represent α and β spin densities, respectively. Reprinted with permission from Ref. [61], Wiley-VCH, 2023.




**Scheme 4.** Synthesis of **5b**$^{+}$·TfO$^{-}$.

**5b**$^{+}$·TfO$^{-}$ was stable in a glove box under argon atmosphere in the solid state and even in solution under air. Single crystals of **5b**$^{+}$·TfO$^{-}$ obtained by recrystallization from a dichloromethane–hexane solution in a degassed sealed tube had an almost $D_{3h}$ symmetric main core structure with similar lengths of C–C bonds to **1c** (Figure 9a). ESR spectra of the benzene solution of **5b**$^{+}$·TfO$^{-}$ at room temperature showed a signal split by six α-protons and a nitrogen atom (Figure 9b). The experimental spin density of α-carbon atoms (0.300) agreed well with the calculated spin density (+0.281, Figure 8c) and that of **1c**. **5b**$^{+}$·TfO$^{-}$, which also showed a weak forbidden transition of $\Delta M_s = \pm 2$, and its triplet state was confirmed by the 2D-ESTN spectrum.

Magnetic susceptibility measurements showed that $\chi_p T$ of **5b**$^{+}$·TfO$^{-}$ was 0.97 emu K mol$^{-1}$, which is very close to the theoretical value (1.00 emu K mol$^{-1}$) of the triplet diradical (Figure 9c). The $\chi_p T$ value was constant at 50–300 K, indicating that **5b**$^{+}$·TfO$^{-}$ has a triplet ground state with a large $\Delta E_{ST}$, as expected from the calculated $\Delta E_{ST}$ of +51.6 kJ mol$^{-1}$ (UB3LYP/6-311G(d,p)).

Although **5b**$^{+}$·TfO$^{-}$ has magnetic properties similar to **1c**, its optical properties are significantly different. **5b**$^{+}$·TfO$^{-}$ showed an NIR absorption band of 815 nm in $CH_2Cl_2$ (Figure 9d), which was assigned to the transition from degenerate α-HOMOs to α-LUMO, which is longer and stronger than the transitions from α-HOMO to α-LUMO and β-HOMO to β-LUMO of **1c** (Figure 7c). Because **1c** is an alternant hydrocarbon, its $T_0$ to $T_1$ transition is symmetry-forbidden, while the nitrogen cation of **5b**$^{+}$ breaks the alternancy symmetry and allows the $T_0$ to $T_1$ transition. In addition, the nitrogen cation lowers the energy level of α-LUMO and reduces the energy difference between α-HOMO and α-LUMO, which causes the longer-wavelength shift of the $T_0$ to $T_1$ transition. Furthermore, **5b**$^{+}$·TfO$^{-}$ exhibited

an NIR fluorescence at 846 nm in $CH_2Cl_2$ (Figure 9d), which is the first example of an NIR-light emissive triplet diradical [63,64].

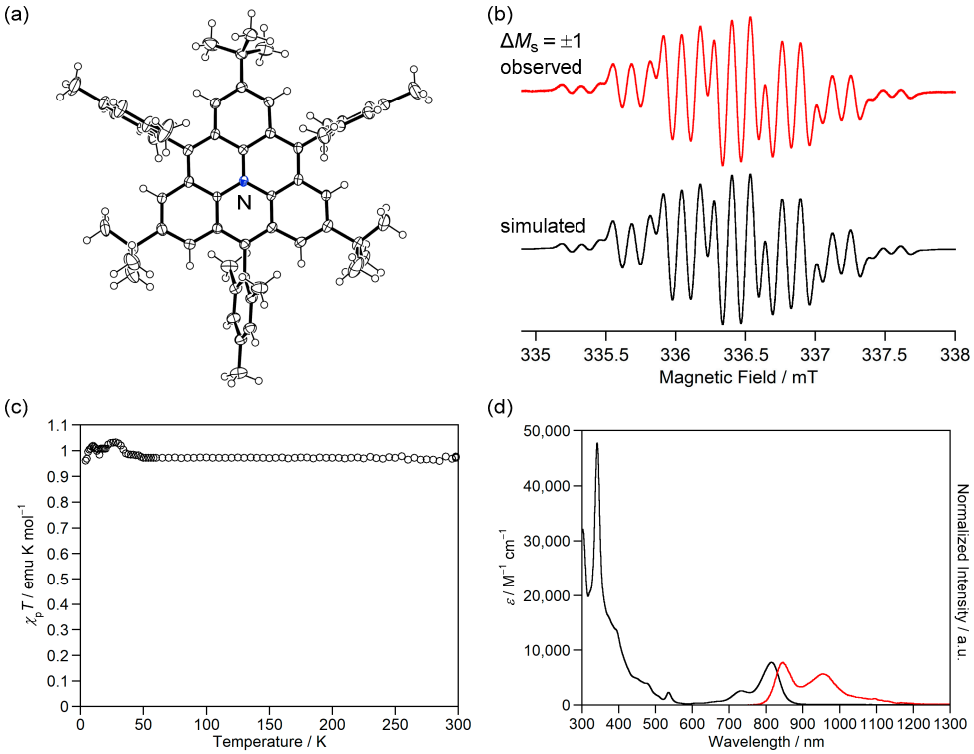



**Figure 9.** (**a**) ORTEP drawing of **5b**$^+$·TfO$^-$. Displacement ellipsoids are drawn at the 50% probability level. TfO$^-$ is omitted for clarity. (**b**) ESR spectrum of **5b**$^+$·TfO$^-$ in benzene at room temperature. (**c**) $\chi_p T$–$T$ curves of **5b**$^+$·TfO$^-$. (**d**) UV-Vis-NIR absorption (black) and fluorescence (red, excited at 730 nm) spectra of **5b**$^+$·TfO$^-$ in $CH_2Cl_2$. Reprinted with permission from Ref. [61], Wiley-VCH, 2023.

## 5. Triplet Kekulé Hydrocarbon

In contrast to the many studies of triplet non-Kekulé hydrocarbons, including Schlenk's hydrocarbon and its derivatives, few triplet Kekulé hydrocarbons have been studied. 2,2-Dimethyl-2*H*-dibenzo[*cd*,*k*]fluoranthene was generated by McMasters et al. in cryogenic matrices, and its triplet ground state was experimentally confirmed (Figure 10a) [65]. An indeno[1,2-*a*]fluorene derivative **6** was reported by Haley et al. as a *m*-quinodimethane-based plausible triplet Kekulé hydrocarbon (Figure 10b) [66]. Although the triplet ESR signal of **6** was successfully observed ($|D| = 0.021$ cm$^{-1}$), **6** has not been isolated, and its ground state has not been fully elucidated.

In the structures of **3a** and **6**, where both sides of *m*-quinodimethane are bridged with benzene, the difference in the number of Clar's aromatic sextet between the Kekulé and diradical structures is 2. We thought that the bonding interaction between the two unpaired electrons could be further reduced by increasing this difference and designed bisdibenzo[3,4:5,6]cyclohepta[1,2-*a*:2,1-*d*]benzene (**7a**), where both sides of *m*-quinodimethane are bridged with biphenyl (Figure 10c) [67]. Because the number of Clar's aromatic sextet is 2 in the Kekulé structure and 5 in the singlet diradical structure, the difference is 3, the bonding interaction between the two unpaired electrons is very weak, and the open-shell singlet diradical character of the singlet state of **7a** was estimated to be 0.99 (LC-UBLYP/6-311G(d,p)//UB3LYP/6-311G(d,p)). On the other hand, the triplet state of **7a** was stabilized because its spin density was similar to *m*-quinodimethane (Figure 10d). DFT calculations predicted that **7a** would have a triplet ground state with a $\Delta E_{ST}$ of +28.7 kJ mol$^{-1}$ (UB3LYP/6-311G(d,p)).

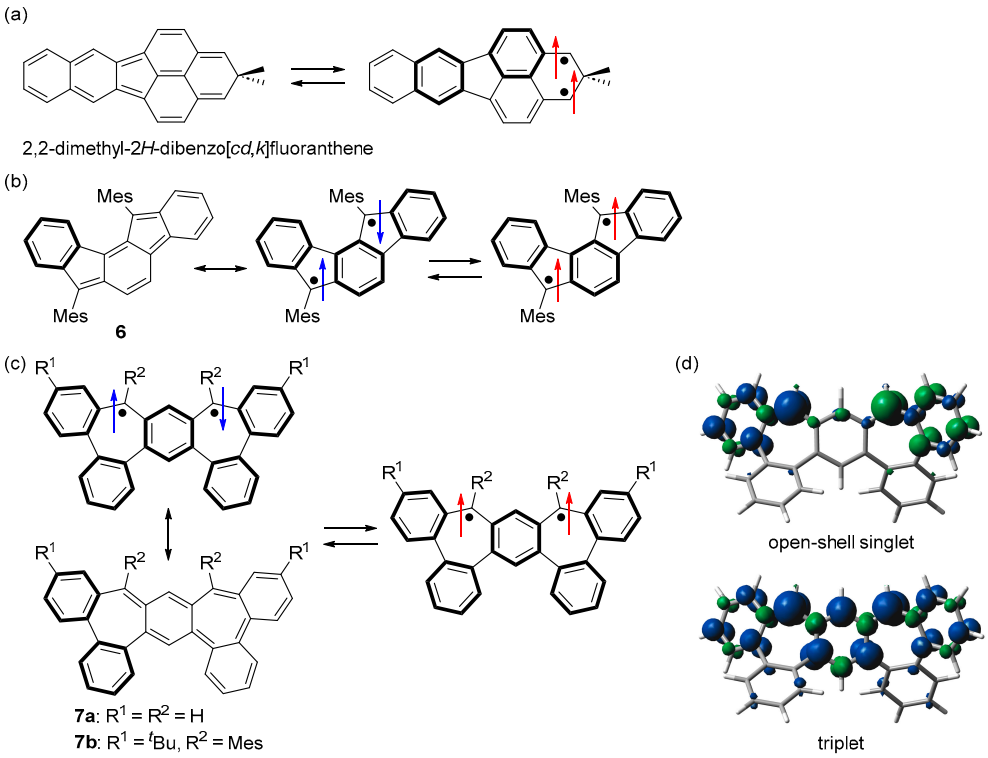
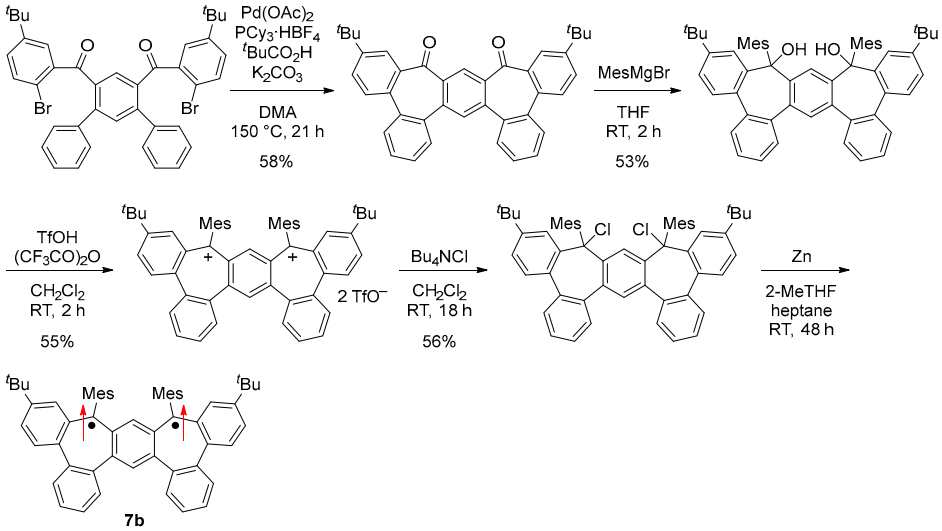



**Figure 10.** Structures of (**a**) 2,2-dimethyl-2*H*-dibenzo[*cd*,*k*]fluoranthene, (**b**) **6**, and (**c**) **7**. Arrows indicate electron spin (blue and red colors are for singlet and triplet diradicals, respectively). (**d**) Spin densities of open-shell singlet and triplet states of **7a**. Blue and green surfaces represent α and β spin densities, respectively.

A kinetically stabilized derivative **7b** was designed and synthesized by introducing *tert*-butyl and mesityl groups for kinetic stabilization (Figure 10c and Scheme 5). Single crystals of **7b** obtained by recrystallization from 2-methyltetrahydrofuran–heptane solution in a degassed sealed tube had an almost $C_2$ symmetric main core structure due to steric repulsion at the *m*-terphenyl moiety.




**Scheme 5.** Synthesis of **7b**. Arrows indicate electron spin.

The Wiberg bond indices of bonds *a* and *b* were close to 1, indicating that these bonds have a single bond character. The HOMA and NICS(1)$_{zz}$ values and the ACID plot of the triplet state of **7a** indicate that ring **A** is weakly aromatic, ring **B** is nonaromatic, and rings

**C** and **D** are aromatic. Therefore, canonical structure **I** with four Clar's aromatic sextets and *m*-quinodimethane moieties contributes significantly, and canonical structure **II** with three Clar's aromatic sextets contributes slightly (Figure 11b).

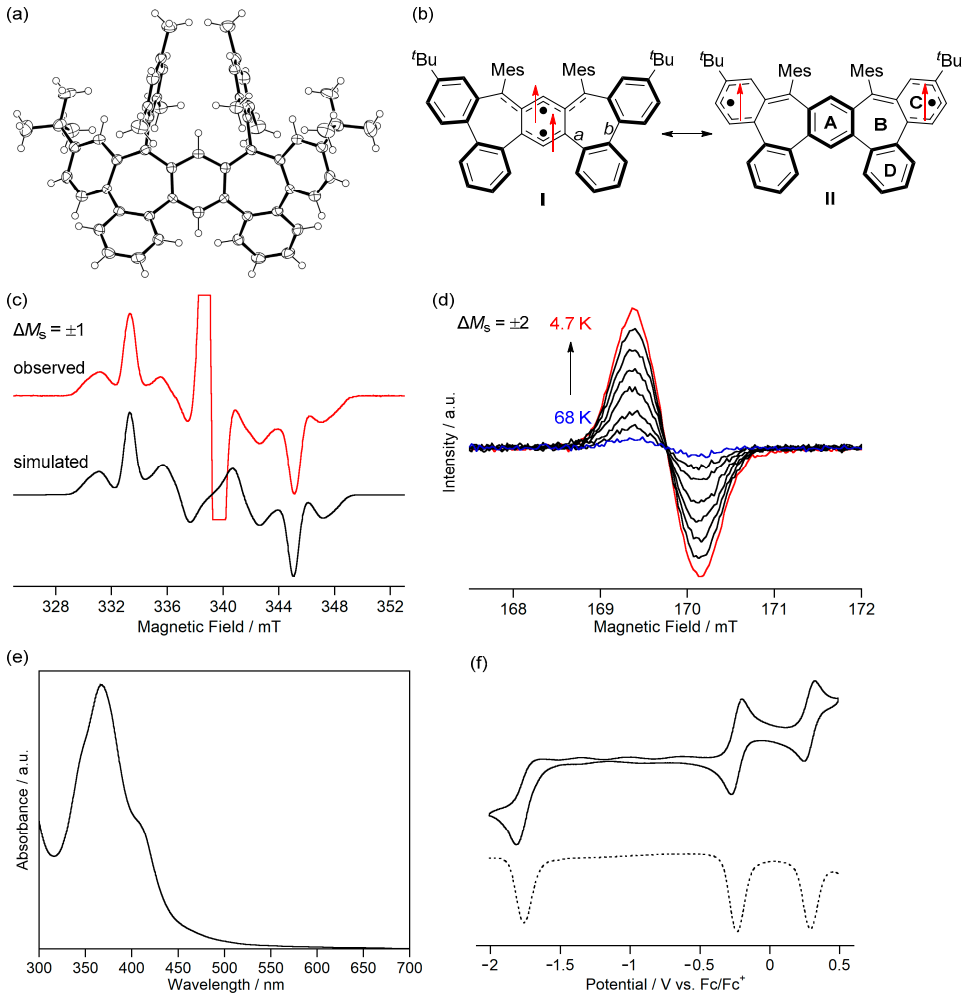



**Figure 11.** (**a**) ORTEP drawing of **7b**. Displacement ellipsoids are drawn at the 50% probability level. (**b**) Resonance structures of **7b**. Arrows indicate electron spin. ESR spectra of **7b** in toluene (**c**) at 69 K and (**d**) from 68 to 4.7 K. (**e**) UV-Vis absorption spectrum of **7b** in $CH_2Cl_2$. (**f**) Cyclic voltammogram (solid line) and differential pulse voltammogram (dashed line) of **7b** in $CH_2Cl_2$. Reprinted with permission from Ref. [67], Wiley-VCH, 2022.

The ESR spectrum of a frozen toluene solution of **7b** showed a signal of the allowed transition with $\Delta M_s = \pm 1$ (Figure 11c). By superimposing the ESR spectra of the two triplet patterns, we found that two conformational isomers existed. The major conformer had zero-field splitting parameters of $|D| = 0.0074$ cm$^{-1}$ and $|E| = 0.0012$ cm$^{-1}$ and the minor conformer had those of $|D| = 0.0083$ cm$^{-1}$ and $|E| = 0.0009$ cm$^{-1}$. Because the $|D|$ values are smaller than the triplet states of **3b** (0.017 cm$^{-1}$) and **6** (0.021 cm$^{-1}$), the two unpaired electrons of **7b** would delocalize over ring **C** (Figure 11b). The signal intensity of the forbidden transition of $\Delta M_s = \pm 2$ increased when the temperature was decreased (Figure 11d). The linear relationship of the triplet signal intensity versus $T^{-1}$ experimentally confirmed the triplet ground state of **7b**.

The fundamental optical and electrochemical properties of **7b** were elucidated by measuring UV-Vis absorption spectra and cyclic voltammograms. **7b** exhibited weak absorption bands below 600 nm in $CH_2Cl_2$, assigned to the transition from α-HOMO to α-LUMO of the triplet state (523 nm, TD-B3LYP/6-311G(d,p)//B3LYP/6-311G(d,p))

(Figure 11e). In addition, **7b** did not show the NIR absorption expected for the open-shell singlet state (956 nm). Therefore, the population of thermally excited singlet states of **7b** at room temperature is negligible, as expected from the calculated $\Delta E_{ST}$ (+26.3 kJ mol$^{-1}$, UB3LYP/6-311G(d,p)). **7b** was unstable in air; when the solution was exposed to air, the absorption of **7b** disappeared within 15 min. The cyclic voltammogram of **7b** showed reversible oxidation waves to radical cation at −0.24 V and to dication at +0.29 V vs. Fc/Fc$^+$ and an irreversible reduction wave to radical anion at −1.82 V (peak potential) (Figure 11f). The small difference between the oxidation potentials would be due to the small energy difference between the α-HOMO (−4.47 eV) and α-HOMO−1 (−4.66 eV). **7b** is the first triplet Kekulé hydrocarbon isolated. The difference in the electronic structures and properties of triplet non-Kekulé hydrocarbons between triplet Kekulé hydrocarbons will be elucidated.

## 6. Conclusions

In this account, studies of *m*-quinodimethane-based polycyclic diradicals, including ideno[2,1-*b*]fluorene (**3a**), an open-shell singlet Kekulé hydrocarbon, azoniadibenzo[*a*,*j*] phenalenide (**4a**), an open-shell singlet zwitterion, triangulene (**1a**) and nitrogen-doped triangulene cation **5a**$^+$, non-Kekulé hydrocarbon-based triplet diradical and diradical cation, and bisdibenzo[3,4:5,6]cyclohepta[1,2-*a*:2,1-*d*]benzene (**7a**), a triplet Kekulé hydrocarbon, are summarized. Kinetically stabilized derivatives of these diradicals were successfully synthesized and isolated, revealing their detailed electronic structures. These diradicals exhibited unique physical properties, such as near-infrared (NIR) absorption/emission, amphoteric redox properties, and a significantly large $\Delta E_{ST}$.

Given the strong correlation between the energy difference between the HOMO and LUMO ($\Delta E_{HL}$, RB3LYP/6-311G(d,p)), the open-shell singlet diradical character of the singlet state, calculated using the open-shell singlet structure (*y*, LC-UBLYP/6-311G(d,p)//UB3LYP/6-311G(d,p)), and the energy difference between the singlet and triplet states ($\Delta E_{ST}$, UB3LYP/6-311G(d,p)) of these *m*-quinodimethane-based polycyclic diradicals (Table 1), controlling the interaction between the two unpaired electrons of *m*-quinodimethane through appropriate molecular design would produce polycyclic diradicals with various *y* and $\Delta E_{ST}$. These studies could pave the way for the development of functional organic materials based on polycyclic diradicals, a promising avenue for future research and applications.

**Table 1.** $\Delta E_{HL}$, *y*, and $\Delta E_{HL}$ of *m*-quinodimethane-based polycyclic diradicals.

| | $\Delta E_{HL}$/kJ mol$^{-1}$ [a] | *Y* [b] | $\Delta E_{ST}$/kJ mol$^{-1}$ [c] |
|---|---|---|---|
| **4a** | 1.54 | 0.57 | −24.1 |
| **3a** | 1.35 | 0.71 | −11.3 |
| **7a** | 0.61 | 0.99 | +28.7 |
| **5a**$^+$ | 0.17 | 0.98 | +53.5 |
| **1a** | 0.09 | 1.00 | +55.9 |

[a] Calculated for closed-shell singlet state at the RB3LYP/6-311G(d,p) level of approximation. [b] Calculated at the LC-UBLYP/6-311G(d,p)//UB3LYP/6-311G(d,p) level of approximation. [c] Calculated at the UB3LYP/6-311G(d,p) level of approximation.

**Funding:** This work was partially supported by JSPS KAKENHI, grant number JP23H01951, and JST CREST, grant number JPMJCR20R3.

**Acknowledgments:** The author is grateful to Yoshito Tobe and Ryo Shintani (Osaka University) for valuable discussion, the late Masayoshi Nakano and Ryohei Kishi (Osaka University) for quantum chemical calculations, Daisuke Shiomi, Kazunobu Sato, and Takeji Takui (Osaka Metropoli-

tan University) for magnetic measurements, Ichiro Hisaki, Mikiji Miyata (Osaka University), and Hiroyasu Sato (Rigaku Corporation) for X-ray crystallographic analysis, Hikaru Sotome, Hiroshi Miyasaka (Osaka University), Masahito Murai, and Shigehiro Yamaguchi (Nagoya University) for optical measurements.

**Conflicts of Interest:** The author declares no conflicts of interest.

## References

1. Abe, M. Diradicals. *Chem. Rev.* **2013**, *113*, 7011–7088. [CrossRef] [PubMed]
2. Sun, Z.; Ye, Q.; Chi, C.; Wu, J. Low band gap polycyclic hydrocarbons: From closed-shell near infrared dyes and semiconductors to open-shell radicals. *Chem. Soc. Rev.* **2012**, *41*, 7857–7889. [CrossRef]
3. Zeng, Z.; Shi, X.; Chi, C.; López Navarrete, J.T.; Casado, J.; Wu, J. Pro-aromatic and anti-aromatic π-conjugated molecules: An irresistible wish to be diradicals. *Chem. Soc. Rev.* **2015**, *44*, 6578–6596. [CrossRef] [PubMed]
4. Kubo, T. Recent Progress in Quinoidal Singlet Biradical Molecules. *Chem. Lett.* **2015**, *44*, 111–122. [CrossRef]
5. Konishi, A.; Kubo, T. Benzenoid Quinodimethanes. *Top. Curr. Chem.* **2017**, *375*, 83. [CrossRef] [PubMed]
6. Tobe, Y. Quinodimethanes Incorporated in Non-Benzenoid Aromatic or Antiaromatic Frameworks. *Top. Curr. Chem.* **2018**, *376*, 12. [CrossRef]
7. Dressler, J.J.; Haley, M.M. Learning how to fine-tune diradical properties by structure refinement. *J. Phys. Org. Chem.* **2020**, *33*, e4114. [CrossRef]
8. Konishi, A.; Yasuda, M. Breathing New Life into Nonalternant Hydrocarbon Chemistry: Syntheses and Properties of Polycyclic Hydrocarbons Containing Azulene, Pentalene, and Heptalene Frameworks. *Chem. Lett.* **2021**, *50*, 195–212. [CrossRef]
9. Shu, C.; Yang, Z.; Rajca, A. From Stable Radicals to Thermally Robust High-Spin Diradicals and Triradicals. *Chem. Rev.* **2023**, *123*, 11954–12003. [CrossRef]
10. Thiele, J.; Balhorn, H. Ueber einen chinoïden Kohlenwasserstoff. *Berichte Dtsch. Chem. Ges.* **1904**, *37*, 1463–1470. [CrossRef]
11. Tschitschibabin, A.E. Über einige phenylierte Derivate des *p*,*p*-Ditolyls. *Berichte Dtsch. Chem. Ges.* **1907**, *40*, 1810–1819. [CrossRef]
12. Montgomery, L.K.; Huffman, J.C.; Jurczak, E.A.; Grendze, M.P. The molecular structures of Thiele's and Chichibabin's hydrocarbons. *J. Am. Chem. Soc.* **1986**, *108*, 6004–6011. [CrossRef] [PubMed]
13. Kubo, T.; Shimizu, A.; Sakamoto, M.; Uruichi, M.; Yakushi, K.; Nakano, M.; Shiomi, D.; Sato, K.; Takui, T.; Morita, Y.; et al. Synthesis, Intermolecular Interaction, and Semiconductive Behavior of a Delocalized Singlet Biradical Hydrocarbon. *Angew. Chem. Int. Ed.* **2005**, *44*, 6564–6568. [CrossRef] [PubMed]
14. Kubo, T.; Shimizu, A.; Uruichi, M.; Yakushi, K.; Nakano, M.; Shiomi, D.; Sato, K.; Takui, T.; Morita, Y.; Nakasuji, K. Singlet Biradical Character of Phenalenyl-Based Kekulé Hydrocarbon with Naphthoquinoid Structure. *Org. Lett.* **2007**, *9*, 81–84. [CrossRef] [PubMed]
15. Shimizu, A.; Uruichi, M.; Yakushi, K.; Matsuzaki, H.; Okamoto, H.; Nakano, M.; Hirao, Y.; Matsumoto, K.; Kurata, H.; Kubo, T. Resonance Balance Shift in Stacks of Delocalized Singlet Biradicals. *Angew. Chem. Int. Ed.* **2009**, *48*, 5482–5486. [CrossRef]
16. Shimizu, A.; Kubo, T.; Uruichi, M.; Yakushi, K.; Nakano, M.; Shiomi, D.; Sato, K.; Takui, T.; Hirao, Y.; Matsumoto, K.; et al. Alternating Covalent Bonding Interactions in a One-Dimensional Chain of a Phenalenyl-Based Singlet Biradical Molecule Having Kekulé Structures. *J. Am. Chem. Soc.* **2010**, *132*, 14421–14428. [CrossRef]
17. Shimizu, A.; Hirao, Y.; Matsumoto, K.; Kurata, H.; Kubo, T.; Uruichi, M.; Yakushi, K. Aromaticity and π-bond covalency: Prominent intermolecular covalent bonding interaction of a Kekulé hydrocarbon with very significant singlet biradical character. *Chem. Commun.* **2012**, *48*, 5629–5631. [CrossRef]
18. Clar, E.; Lang, K.F.; Schulz-Kiesow, H. Aromatische Kohlenwasserstoffe, LXX. Mitteil.[1)]: Zethren (1.12; 6.7-Dibenztetracen). *Chem. Berichte* **1955**, *88*, 1520–1527. [CrossRef]
19. Wu, T.-C.; Chen, C.-H.; Hibi, D.; Shimizu, A.; Tobe, Y.; Wu, Y.-T. Synthesis, Structure, and Photophysical Properties of Dibenzo[*de*,*mn*]naphthacenes. *Angew. Chem. Int. Ed.* **2010**, *49*, 7059–7062. [CrossRef]
20. Umeda, R.; Hibi, D.; Miki, K.; Tobe, Y. Tetradehydrodinaphtho[10]annulene: A Hitherto Unknown Dehydroannulene and a Viable Precursor to Stable Zethrene Derivatives. *Org. Lett.* **2009**, *11*, 4104–4106. [CrossRef]
21. Clar, E.; Macpherson, I.A. The significance of Kekulé structures for the stability of aromatic systems—II. *Tetrahedron* **1962**, *18*, 1411–1416. [CrossRef]
22. Li, Y.; Heng, W.-K.; Lee, B.S.; Aratani, N.; Zafra, J.L.; Bao, N.; Lee, R.; Sung, Y.M.; Sun, Z.; Huang, K.-W.; et al. Kinetically Blocked Stable Heptazethrene and Octazethrene: Closed-Shell or Open-Shell in the Ground State? *J. Am. Chem. Soc.* **2012**, *134*, 14913–14922. [CrossRef]
23. Hu, P.; Lee, S.; Herng, T.S.; Aratani, N.; Gonçalves, T.P.; Qi, Q.; Shi, X.; Yamada, H.; Huang, K.-W.; Ding, J.; et al. Toward Tetraradicaloid: The Effect of Fusion Mode on Radical Character and Chemical Reactivity. *J. Am. Chem. Soc.* **2016**, *138*, 1065–1077. [CrossRef]

24. Huang, R.; Phan, H.; Herng, T.S.; Hu, P.; Zeng, W.; Dong, S.; Das, S.; Shen, Y.; Ding, J.; Casanova, D.; et al. Higher Order π-Conjugated Polycyclic Hydrocarbons with Open-Shell Singlet Ground State: Nonazethrene versus Nonacene. *J. Am. Chem. Soc.* **2016**, *138*, 10323–10330. [CrossRef]
25. Chase, D.T.; Rose, B.D.; McClintock, S.P.; Zakharov, L.N.; Haley, M.M. Indeno[1,2-*b*]fluorenes: Fully Conjugated Antiaromatic Analogues of Acenes. *Angew. Chem. Int. Ed.* **2011**, *50*, 1127–1130. [CrossRef]
26. Chase, D.T.; Fix, A.G.; Kang, S.J.; Rose, B.D.; Weber, C.D.; Zhong, Y.; Zakharov, L.N.; Lonergan, M.C.; Nuckolls, C.; Haley, M.M. 6,12-Diarylindeno[1,2-*b*]fluorenes: Syntheses, Photophysics, and Ambipolar OFETs. *J. Am. Chem. Soc.* **2012**, *134*, 10349–10352. [CrossRef] [PubMed]
27. Barker, J.E.; Frederickson, C.K.; Jones, M.H.; Zakharov, L.N.; Haley, M.M. Synthesis and Properties of Quinoidal Fluorenofluorenes. *Org. Lett.* **2017**, *19*, 5312–5315. [CrossRef] [PubMed]
28. Rudebusch, G.E.; Zafra, J.L.; Jorner, K.; Fukuda, K.; Marshall, J.L.; Arrechea-Marcos, I.; Espejo, G.L.; Ponce Ortiz, R.; Gómez-García, C.J.; Zakharov, L.N.; et al. Diindeno-fusion of an anthracene as a design strategy for stable organic biradicals. *Nat. Chem.* **2016**, *8*, 753–759. [CrossRef]
29. Iwashita, S.; Ohta, E.; Higuchi, H.; Kawai, H.; Fujiwara, K.; Ono, K.; Takenaka, M.; Suzuki, T. First stable 7,7,8,8-tetraaryl-*o*-quinodimethane: Isolation, X-ray structure, electrochromic response of 9,10-bis(dianisylmethylene)-9,10-dihydrophenanthrene. *Chem. Commun.* **2004**, 2076–2077. [CrossRef]
30. Shimizu, A.; Tobe, Y. Indeno[2,1-*a*]fluorene: An Air-Stable *ortho*-Quinodimethane Derivative. *Angew. Chem. Int. Ed.* **2011**, *50*, 6906–6910. [CrossRef]
31. Schlenk, W.; Brauns, M. Zur Frage der Metachinoide. *Berichte Dtsch. Chem. Ges.* **1915**, *48*, 661–669. [CrossRef]
32. Kothe, G.; Denkel, K.; Sümmermann, W. *Schlenk's* Biradical.—A Molecule in the Triplet Ground State. *Angew. Chem. Int. Ed. Engl.* **1970**, *9*, 906–907. [CrossRef]
33. Rajca, A.; Utamapanya, S.; Xu, J. Control of magnetic interactions in polyarylmethyl triplet diradicals using steric hindrance. *J. Am. Chem. Soc.* **1991**, *113*, 9235–9241. [CrossRef]
34. Rajca, A.; Utamapanya, S. π-Conjugated systems with unique electronic structure: A case of planarized 1,3-connected polyarylmethyl carbodianion and stable triplet hydrocarbon diradical. *J. Org. Chem.* **1992**, *57*, 1760–1767. [CrossRef]
35. Clar, E.; Stewart, D.G. Aromatic Hydrocarbons. LXV. Triangulene Derivatives[1]. *J. Am. Chem. Soc.* **1953**, *75*, 2667–2673. [CrossRef]
36. Clar, E.; Stewart, D.G. Aromatic Hydrocarbons. LXVIII. Triangulene Derivatives. Part II[1]. *J. Am. Chem. Soc.* **1954**, *76*, 3504–3507. [CrossRef]
37. Inoue, J.; Fukui, K.; Kubo, T.; Nakazawa, S.; Sato, K.; Shiomi, D.; Morita, Y.; Yamamoto, K.; Takui, T.; Nakasuji, K. The First Detection of a Clar's Hydrocarbon, 2,6,10-Tri-*tert*-Butyltriangulene: A Ground-State Triplet of Non-Kekulé Polynuclear Benzenoid Hydrocarbon. *J. Am. Chem. Soc.* **2001**, *123*, 12702–12703. [CrossRef]
38. Li, Y.; Huang, K.; Sun, Z.; Webster, R.; Zeng, Z.; Zeng, W.; Chi, C.; Furukawa, K.; Wu, J. A kinetically blocked 1,14:11,12-dibenzopentacene: A persistent triplet diradical of a non-Kekulé polycyclic benzenoid hydrocarbon. *Chem. Sci.* **2014**, *5*, 1908–1914. [CrossRef]
39. Shimizu, A.; Arikawa, S.; Morikoshi, T.; Shintani, R. *m*-Quinodimethane-based fused-ring triplet hydrocarbons. *Pure Appl. Chem.* **2023**, *95*, 401–412. [CrossRef]
40. Shimizu, A.; Kishi, R.; Nakano, M.; Shiomi, D.; Sato, K.; Takui, T.; Hisaki, I.; Miyata, M.; Tobe, Y. Indeno[2,1-*b*]fluorene: A 20-π-Electron Hydrocarbon with Very Low-Energy Light Absorption. *Angew. Chem. Int. Ed.* **2013**, *52*, 6076–6079. [CrossRef]
41. Miyoshi, H.; Miki, M.; Hirano, S.; Shimizu, A.; Kishi, R.; Fukuda, K.; Shiomi, D.; Sato, K.; Takui, T.; Hisaki, I.; et al. Fluoreno[2,3-*b*]fluorene vs Indeno[2,1-*b*]fluorene: Unusual Relationship between the Number of π Electrons and Excitation Energy in *m*-Quinodimethane-Type Singlet Diradicaloids. *J. Org. Chem.* **2017**, *82*, 1380–1388. [CrossRef]
42. Jiang, Q.; Wang, L.; Wei, H.; Peng, Y.; Xu, G.; Li, Z.; Liu, P.; Hu, Z.; Niu, W.; Chen, Y.; et al. A Kinetically Stabilized Dianthraceno[2,3-*a*:3′,2′-*h*]-*s*-Indacene: Stable Kekule Diradical Polycyclic Hydrocarbon with Triplet Ground State, *Angew. Chem. Int. Ed.* **2024**, e202422994. [CrossRef]
43. Abe, M.; Adam, W.; Nau, W.M. Photochemical Generation and Methanol Trapping of Localized 1,3 and 1,4 Singlet Diradicals Derived from a Spiroepoxy-Substituted Cyclopentane-1,3-diyl. *J. Am. Chem. Soc.* **1998**, *120*, 11304–11310. [CrossRef]
44. Niecke, E.; Fuchs, A.; Baumeister, F.; Nieger, M.; Schoeller, W.W. A $P_2C_2$ Four-Membered Ring with Unusual Bonding—Synthesis, Structure, and Ring Opening of a 1,3-Diphosphacyclobutane-2,4-diyl. *Angew. Chem. Int. Ed. Engl.* **1995**, *34*, 555–557. [CrossRef]
45. Arikawa, S.; Shimizu, A.; Shintani, R. Azoniadibenzo[*a,j*]phenalenide: A Polycyclic Zwitterion with Singlet Biradical Character. *Angew. Chem. Int. Ed.* **2019**, *58*, 6415–6419. [CrossRef] [PubMed]
46. Kruszewski, J.; Krygowski, T.M. Definition of aromaticity basing on the harmonic oscillator model. *Tetrahedron Lett.* **1972**, *13*, 3839–3842. [CrossRef]
47. Krygowski, T.M. Crystallographic studies of inter- and intramolecular interactions reflected in aromatic character of .pi.-electron systems. *J. Chem. Inf. Model.* **1993**, *33*, 70–78.

48. Schleyer, P.V.R.; Maerker, C.; Dransfeld, A.; Jiao, H.; van Eikema Hommes, N.J.R. Nucleus-Independent Chemical Shifts: A Simple and Efficient Aromaticity Probe. *J. Am. Chem. Soc.* **1996**, *118*, 6317–6318. [CrossRef]
49. Chen, Z.; Wannere, C.S.; Corminboeuf, C.; Puchta, R.; Schleyer, P.V.R. Nucleus-Independent Chemical Shifts (NICS) as an Aromaticity Criterion. *Chem. Rev.* **2005**, *105*, 3842–3888. [CrossRef]
50. Schleyer, P.V.R.; Manoharan, M.; Wang, Z.-X.; Kiran, B.; Jiao, H.; Puchta, R.; van Eikema Hommes, N.J.R. Dissected Nucleus-Independent Chemical Shift Analysis of π-Aromaticity and Antiaromaticity. *Org. Lett.* **2001**, *16*, 2465–2468. [CrossRef]
51. Herges, R.; Geuenich, D. Delocalization of Electrons in Molecules. *J. Phys. Chem. A* **2001**, *105*, 3214–3220. [CrossRef]
52. Geuenich, D.; Hess, K.; Köhler, F.; Herges, R. Anisotropy of the Induced Current Density (ACID), a General Method to Quantify and Visualize Electronic Delocalization. *Chem. Rev.* **2005**, *105*, 3758–3772. [CrossRef] [PubMed]
53. Horii, K.; Kishi, R.; Nakano, M.; Shiomi, D.; Sato, K.; Takui, T.; Konishi, A.; Yasuda, M. Bis-periazulene (Cyclohepta[*def*]fluorene) as a Nonalternant Isomer of Pyrene: Synthesis and Characterization of Its Triaryl Derivatives. *J. Am. Chem. Soc.* **2022**, *144*, 3370–3375. [CrossRef]
54. Pavliček, N.; Mistry, A.; Majzik, Z.; Moll, N.; Meyer, G.; Fox, D.J.; Gross, L. Synthesis and characterization of triangulene. *Nat. Nanotechnol.* **2017**, *12*, 308–312. [CrossRef] [PubMed]
55. Su, X.; Li, C.; Du, Q.; Tao, K.; Wang, S.; Yu, P. Atomically Precise Synthesis and Characterization of Heptauthrene with Triplet Ground State. *Nano Lett.* **2020**, *20*, 6859–6864. [CrossRef]
56. Arikawa, S.; Shimizu, A.; Shiomi, D.; Sato, K.; Shintani, R. Synthesis and Isolation of a Kinetically Stabilized Crystalline Triangulene. *J. Am. Chem. Soc.* **2021**, *143*, 19599–19605. [CrossRef]
57. Wiberg, K.B. Application of the pople-santry-segal CNDO method to the cyclopropylcarbinyl and cyclobutyl cation and to bicyclobutane. *Tetrahedron* **1968**, *24*, 1083–1096. [CrossRef]
58. Valenta, L.; Mayländer, M.; Kappeler, P.; Blacque, O.; Šolomek, T.; Richert, S.; Juríček, M. Trimesityltriangulene: A persistent derivative of Clar's hydrocarbon. *Chem. Commun.* **2022**, *58*, 3019–3022. [CrossRef]
59. Astashkin, A.V.; Schweiger, A. Electron-spin transient nutation: A new approach to simplify the interpretation of ESR spectra. *Chem. Phys. Lett.* **1990**, *174*, 595–602. [CrossRef]
60. Sato, K.; Yano, M.; Furuichi, M.; Shiomi, D.; Takui, T.; Abe, K.; Itoh, K.; Higuchi, A.; Katsuma, K.; Shirota, Y. Polycationic High-Spin States of One- and Two-Dimensional (Diarylamino)benzenes, Prototypical Model Units for Purely Organic Ferromagnetic Metals as Studied by Pulsed ESR/Electron Spin Transient Nutation Spectroscopy. *J. Am. Chem. Soc.* **1997**, *119*, 6607–6613. [CrossRef]
61. Arikawa, S.; Shimizu, A.; Shiomi, D.; Sato, K.; Takui, T.; Sotome, H.; Miyasaka, H.; Murai, M.; Yamaguchi, S.; Shintani, R. A Kinetically Stabilized Nitrogen-Doped Triangulene Cation: Stable and NIR Fluorescent Diradical Cation with Triplet Ground State. *Angew. Chem. Int. Ed.* **2023**, *62*, e202302714. [CrossRef] [PubMed]
62. Wang, T.; Berdonces-Layunta, A.; Friedrich, N.; Vilas-Varela, M.; Calupitan, J.P.; Pascual, J.I.; Pena, D.; Casanova, D.; Corso, M.; de Oteyza, D.G. Aza-Triangulene: On-Surface Synthesis and Electronic and Magnetic Properties. *J. Am. Chem. Soc.* **2022**, *144*, 4522–4529. [CrossRef] [PubMed]
63. Namai, H.; Ikeda, H.; Hoshi, Y.; Kato, N.; Morishita, Y.; Mizuno, K. Thermoluminescence and a New Organic Light-Emitting Diode (OLED) Based on Triplet−Triplet Fluorescence of the Trimethylenemethane (TMM) Biradical. *J. Am. Chem. Soc.* **2007**, *129*, 9032–9036. [CrossRef] [PubMed]
64. Feng, Z.; Chong, Y.; Tang, S.; Fang, Y.; Zhao, Y.; Jiang, J.; Wang, X. A stable triplet diradical emitter. *Chem. Sci.* **2021**, *12*, 15151–15156. [CrossRef]
65. McMasters, D.R.; Wirz, J. Spectroscopy and Reactivity of Kekulé Hydrocarbons with Very Small Singlet−Triplet Gaps. *J. Am. Chem. Soc.* **2001**, *123*, 238–246. [CrossRef]
66. Dressler, J.J.; Zhou, Z.; Marshall, J.L.; Kishi, R.; Takamuku, S.; Wei, Z.; Spisak, S.N.; Nakano, M.; Petrukhina, M.A.; Haley, M.M. Synthesis of the Unknown Indeno [1,2-*a*]fluorene Regioisomer: Crystallographic Characterization of Its Dianion. *Angew. Chem. Int. Ed.* **2017**, *56*, 15363–15367. [CrossRef]
67. Shimizu, A.; Morikoshi, T.; Sugisaki, K.; Shiomi, D.; Sato, K.; Takui, T.; Shintani, R. Synthesis and Isolation of a Kekulé Hydrocarbon with a Triplet Ground State. *Angew. Chem. Int. Ed.* **2022**, *61*, e202205729. [CrossRef]


**Disclaimer/Publisher's Note:** The statements, opinions and data contained in all publications are solely those of the individual author(s) and contributor(s) and not of MDPI and/or the editor(s). MDPI and/or the editor(s) disclaim responsibility for any injury to people or property resulting from any ideas, methods, instructions or products referred to in the content.